Volume 24, No 3 | International Journal of Radiation Research, July 2026

Application of ultrasound-based thyroid imaging reporting and data system for assessing thyroid nodules with suspected malignancy

Y. Wu[1#], D. Liu[2#], Y. Zhou[1], X. Xin[3], A. Guo[1*]

[1]*Physical Examination Center, The Second Hospital of Hebei Medical University, Shijiazhuang 050000, Hebei Province, China*

[2]*Mathematics teaching and research department of medical imaging college Center, The Second Hospital of Hebei Medical University, Shijiazhuang 050031, Hebei Province, China*

[3]*Department of Reproductive Medicine, The Second Hospital of Hebei Medical University, Shijiazhuang 050000, Hebei Province, China*

► ***Original article***

Corresponding author:
Ainan Guo, M.M.,
E-mail: *ainanguo902@163.com*

Received: April 2025
Final revised: February 2026
Accepted: April 2026

Int. J. Radiat. Res., July 2026; 24(3): 789-794

DOI: 10.61186/ijrr.24.3.28

Keywords: *Thyroid nodule, microcarcinomas, ultrasonography, classification system, diagnosis, differential, retrospective studies.*

#These authors contributed equally in this work.

ABSTRACT

Background: To evaluate the effectiveness of the Kwak Thyroid Imaging Reporting and Data System (TI-RADS) in preoperatively identifying suspicious malignant thyroid nodules (MTNs) and to investigate size-dependent ultrasound features associated with malignancy. ***Materials and Methods:*** This study reviewed 155 patients (212 nodules suspected of thyroid cancer) who underwent surgical treatment at The Second Hospital of Hebei Medical University between June 2015 and December 2019. Preoperative ultrasound findings were classified using the Kwak TI-RADS system based on five features: solid composition, hypoechogenicity, irregular/lobulated margin, aspect ratio ≥1, and microcalcifications. Nodules were categorized into TI-RADS 3–5, with histopathology serving as the diagnostic benchmark. The positive predictive value (PPV), sensitivity, specificity, negative predictive value (NPV), and accuracy were calculated. Additionally, ultrasonographic characteristics of papillary malignant nodules (≤1 cm) were compared to those of larger malignant nodules (>1 cm). ***Results:*** Of the 212 nodules, histopathology identified 193 as malignant and 19 as benign. The TI-RADS demonstrated a PPV of 96.94%, sensitivity of 98.45%, specificity of 68.42%, NPV of 81.25%, and accuracy of 95.75%. Size-stratified analysis revealed distinct imaging phenotypes: microcarcinomas (n = 119) were more frequently associated with an aspect ratio ≥1 (80.67%) and microcalcifications (57.98%), while larger malignant nodules (n = 74) exhibited higher rates of coarse calcifications (24.32%) and increased vascularity (grade 2/3: 32.43%). The two groups showed significant differences in aspect ratio, type of calcification, and vascularity (p<0.01). ***Conclusion:*** The TI RADS classification effectively predicts the diagnosis of suspicious MTN.

INTRODUCTION

In endocrinology, thyroid nodules (TNs) are a common clinical condition, with prevalence rates reported between 20% and 76% in the general population. Among these nodules, malignant thyroid nodules (MTNs) represent about 5% to 15%, and are mainly comprised of papillary, follicular, and medullary carcinoma [1-4]. High-resolution ultrasound has significantly increased the detection rate of TNs. However, confidently distinguishing between benign and MTNs remains a clinical challenge [1, 5]. Ultrasound is the preferred imaging modality for the evaluation of TNs due to its non-invasive nature, convenience, and high reproducibility[6]. This technique can clearly depict nodule morphology, margins, echogenicity, calcification patterns, and vascularity [7, 8]. However, conventional ultrasound diagnosis relies heavily on the operator's experience, making it prone to significant subjectivity and variability between different observers [9]. To enhance consistency and facilitate clinical decision-making, various ultrasound reporting systems have been developed. Among these, the Thyroid Imaging Reporting and Data System (TI-RADS) proposed by Kwak has emerged as a widely utilized tool for risk stratification [10]. The TI-RADS is a risk-stratification guideline based on B-mode ultrasound features [11]. Several versions of the TI-RADS have been proposed to date, including those by Kwak, the American College of Radiology, the European Thyroid Association, and the Chinese Thyroid Association. These systems assign scores to TNs based on key B-mode ultrasound features such as margin, composition, calcification, and shape [12]. The application of TI-RADS has been shown to effectively reduce unnecessary interventions while improving the detection of malignant nodules [13].

The novelty of this study lies in the targeted validation and methodological refinement of the Kwak TI-RADS system for preoperatively assessing clinically suspicious MTNs in a Chinese cohort with

histopathological confirmation. While TI-RADS is widely used for general risk stratification, its effectiveness in high-suspicion populations - where diagnostic accuracy is crucial for surgical decision-making - has not been thoroughly characterized. To improve clinical applicability, we proposed a simplified scoring method that combines "solid composition" and "hypoechogenicity" into a single malignancy criterion. This approach streamlines risk assessment for nodules already under strong suspicion. Furthermore, our size-stratified analysis revealed distinct ultrasound phenotypes between papillary thyroid microcarcinomas (≤1 cm) and larger malignant nodules (>1 cm). Specifically, microcarcinomas were more frequently associated with microcalcifications and irregular margins, while larger nodules showed a greater reliance on solid/hypoechogenic architecture and a taller-than-wide shape. These findings offer valuable insights for refining preoperative ultrasound evaluation and facilitating more individualized management of TNs with high malignant potential.

MATERIALS AND METHODS

Clinical case collection

This study retrospectively analyzed 155 patients with TNs confirmed by histopathology who underwent surgical resection at The Second Hospital of Hebei Medical University between June 2015 and December 2019. Clinical data analysis identified a total of 212 suspicious thyroid nodules among these patients. Preoperative conventional ultrasound findings were collected and reviewed for all cases included in the study. The cohort comprised 17 men and 138 women, with ages ranging from 18 to 80 years (mean ± SD: 45.7 ± 12.3 years). Histopathological examination revealed that out of the 212 lesions, 19 were benign and 193 were malignant.

Inclusion criteria: Complete ultrasound data of the patient, the patient's surgical pathology examination confirmed TN, the patient has an ultrasound TI RADS grading report, the age of the patient is between 18 and 80 years and having informed consent.

Exclusion criteria: Patients with pure cystic nodules and with prior thyroid surgery were excluded from the study.

Instruments and methods

Ultrasound examinations were performed using a Philips iU-Elite color Doppler ultrasound system (Philips Healthcare, Bothell, WA, USA) with an L12-5 linear array transducer (5.0-12.0 MHz). Patients were placed in the supine position for optimal visualization of the anterior neck. Conventional two-dimensional and color Doppler ultrasound were used for continuous scanning of the TNs. The size of TNs was quantified, and the longitudinal-to-transverse diameter ratio (L/T) was calculated. The location of the nodule (left lobe, right lobe, isthmus), number (single, multiple), shape (regular, irregular), internal echo (solid hypoechoic, cystic-solid mixed echo), boundary (clear, unclear), presence and type of calcification, presence and region of lymph node metastasis (central, lateral neck, and both), association with adjacent tissue, and blood flow distribution characteristics (grades 0 to 3) were recorded.

Ultrasound diagnostic criteria

We applied the TI-RADS system (Kwak) to distinguish benign from malignant lesions [14, 15]. Indicators such as unclear margins, solid nodules, hypoechogeneity, microcalcifications, and blood supply primarily at the margins suggest the presence of suspicious malignant nodules. The detailed information is shown in table 1. If all indicators are negative, the nodule is classified as grade 3. A single positive indicator results in a grade of 4A, while two positive indicators yield a grade of 4B. A classification of grade 4C is assigned when three to four positive indicators are present. A nodule exhibiting five positive indicators is categorized as grade 5. Nodules classified as grades 3 to 4A are considered benign, whereas those classified as grades 4B to 5 are regarded as malignant.

Table 1. TI RADS classification.

Characteristic	Description
Unclear margins	Cystic or almost completely cystic
	Hemorrhagic
	Cystic-solid mixed
	Solid or almost completely solid
Solid nodules	Anechoic
	Hyper or equal echo
	Hypoechoic
	Markedly hypoechoic
Hypoechogeneity	Smooth or blurred
	Lobulated or irregular
	Extrathyroidal invasion
Microcalcifications	No or large comet tail
	Coarse calcification
	Ring-like (marginal) calcification
	Punctate strong echo
Blood supply primarily	Aspect ratio＜1
	Aspect ratio≥1

The assessment of blood flow intensity during color Doppler ultrasound examination was conducted using the Adler classification: Grade 0 indicates absent vascularity, while grade 1 denotes one or 2 flow signals. Grade 2 corresponds to 3 to 4 spotty flows or 2 major vessels. Grade 3 is assigned to instances involving more than 2 vessels with clearly defined walls.

Histopathological evaluation

All thyroid specimens were procured via surgical resection (lobectomy or total thyroidectomy) due to clinical suspicion of malignancy or progressive nodule growth during follow-up. Final diagnoses

were established based on histopathological examination of formalin-fixed, paraffin-embedded sections. Tissue samples were fixed in 10% formalin, dehydrated in graded ethanol, subjected to xylene clearance, and embedded in paraffin. Sections (5 μm) were prepared and stained with a hematoxylin and eosin (H&E) kit (Cat. No. C0105S, Beyotime Biotechnology, Shanghai, China) following established protocols. Slides were evaluated by two pathologists who were blinded to preoperative ultrasound findings and TI-RADS classifications. Histopathological diagnoses were categorized as benign or malignant, with papillary carcinomas further subclassified based on nuclear characteristics and architectural patterns. The definitive histopathological diagnosis was utilized as the gold standard for TI-RADS assessment.

This retrospective study complied with the Declaration of Helsinki and received approval from the Ethics Committee of The Second Hospital of Hebei Medical University (approval number: 2024-R665; approval date: 11th Oct. 2024).

Statistical analysis

Statistical analyses used SPSS 22.0 (IBM Corp.). Categorical data were compared using the chi-square test, with $p<0.05$ considered significant. The diagnostic performance of TI-RADS for suspicious malignant thyroid nodules was evaluated.

RESULTS

Patient general information and pathological diagnosis

We conducted a retrospective analysis of 155 patients with a total of 212 thyroid nodules. The cohort comprised 17 male and 138 female patients, aged 20–78 years (mean age: 45.7 ± 12.3 years). Among the 212 nodules, 19 were benign and 193 malignant. The 19 benign nodules included 11 right, 6 left, and 2 isthmic; histology: nodular goiter (n=13), follicular adenoma (n=3), thyroid adenoma (n=3). Malignant nodules: 92 right, 76 left, 25 isthmic; histology: papillary thyroid carcinoma (n=190), medullary (n=2), and undifferentiated squamous cell carcinoma (n=1). Detailed distribution and pathological classifications are summarized in table 2.

Representative ultrasound imaging features

Figure 1 presents representative ultrasound features of benign and malignant TNs. The benign nodule (figure 1A) displays a well-circumscribed, homogeneous echotexture without suspicious features such as microcalcifications or irregular margins, consistent with TI-RADS category 3. In contrast, the malignant nodule (>1 cm; figure 1B) shows marked hypoechogenicity, microcalcifications, irregular margins, and a taller-than-wide shape, aligning with TI-RADS 5 criteria. Similarly, the papillary thyroid microcarcinoma (≤1 cm) (figure 1C) shows a hypoechoic lesion with microcalcifications and irregular borders, classified as TI-RADS 4c. These findings underscore the utility of TI-RADS in identifying malignancy indicators across various nodule sizes.

Table 2. General patient data (¯x±s) [n(%)].

Project	Patient (n=155, %)	
Age		45.7±12.3
Gender	Male	17(10.97)
	Female	138(89.03)
	NT(n=212, %)	
Benign nodules	Nodular goiter	13(6.13)
	Follicular adenoma	3(1.42)
	Thyroid adenoma	3(1.42)
Malignant nodules	Papillary thyroid carcinoma	190(89.62)
	Anaplastic thyroid carcinoma	1(0.47)
	Medullary thyroid cancer	2(0.94)

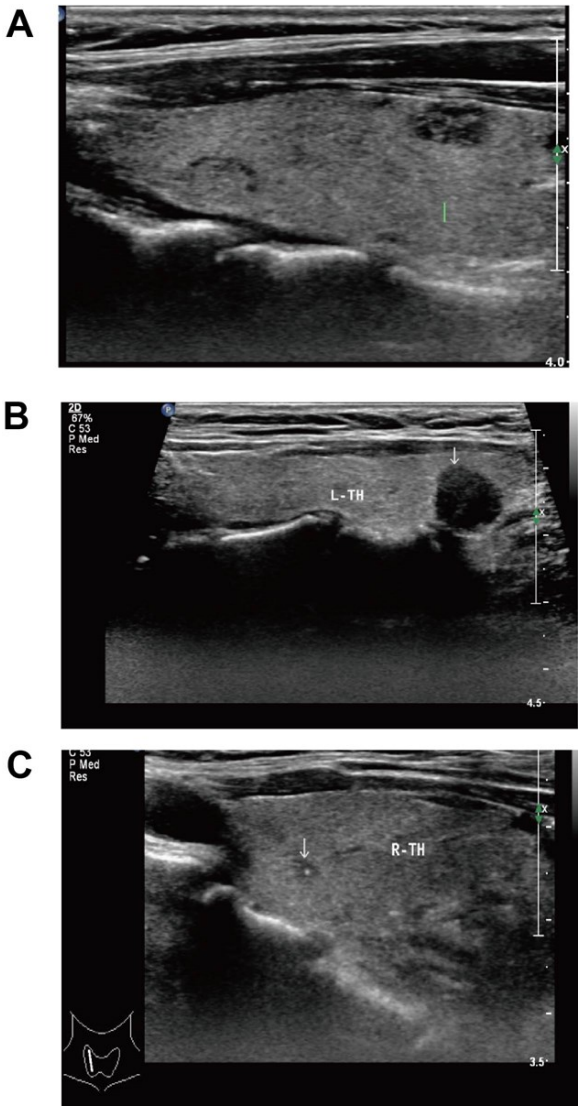


Figure 1. Representative original ultrasound images of thyroid nodules based on TI-RADS classification. **(A)** Benign TNs; **(B)** Malignant TNs; **(C)** Papillary thyroid microcarcinoma.

Representative histopathological findings

To establish the histopathological foundation of our reference standard, figure 2 includes representative H&E-stained sections from surgically resected specimens within our cohort. Panel A displays a papillary thyroid microcarcinoma (≤1 cm) characterized by small follicles and nuclei exhibiting classic features such as nuclear clearing, longitudinal grooves, and intranuclear pseudoinclusions. Panel B illustrates a classical papillary thyroid carcinoma (>1 cm), which shows similar nuclear atypia but with more extensive architectural distortion and papillary formation. Panel C depicts a benign thyroid nodule, demonstrating preserved follicular architecture, uniform epithelial cells, and absence of nuclear atypia - consistent with nodular hyperplasia or adenomatoid nodule. Histopathological diagnoses from pathologists were used as the reference standard to evaluate TI-RADS performance in distinguishing benign from malignant nodules.

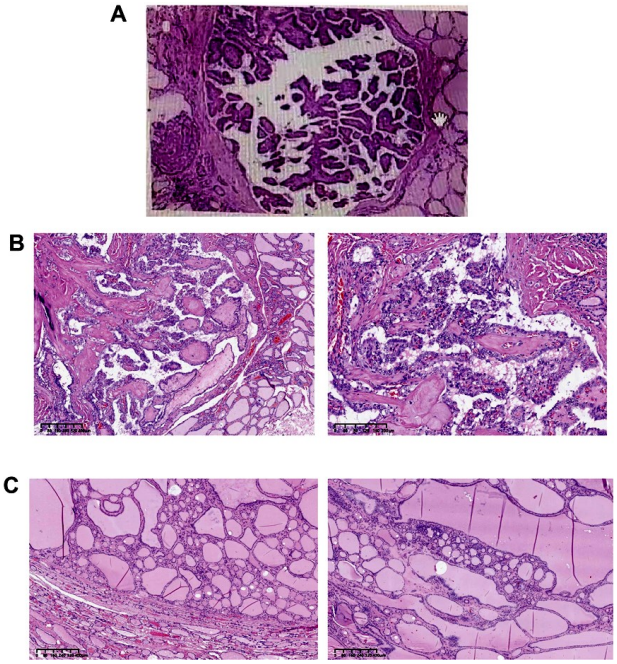


Figure 2. Representative H&E-stained histopathological images of malignant thyroid lesions. **(A)** Papillary thyroid microcarcinoma (≤1 cm): Classic nuclear features including nuclear grooves and intranuclear pseudoinclusions; **(B)** Classical papillary thyroid carcinoma (>1 cm): Marked nuclear atypia, crowded arrangement, and complex papillary structures; **(C)** Benign thyroid nodule: Well-preserved follicular architecture and monomorphic follicular cells without nuclear atypia. Sections were stained using standard hematoxylin and eosin protocols and examined under light microscopy. Magnification: ×400.

TI RADS diagnosis of benign TN

Table 3 shows that among the 19 histopathologically confirmed benign TNs, 6 were >1 cm and 13 measured ≤1 cm. Ultrasound features revealed that 17 nodules (89.47%) were solid with a hypoechoic appearance, while 2 (10.53%) exhibited a mixed cystic-solid pattern. Microcalcifications were present in 13 nodules (68.42%), and coarse calcifications in one (5.26%). Doppler flow assessment indicated grade 1 vascularity in 9 nodules (47.37%), grade 2 in 9 (47.37%), and grade 3 in 1 (5.26%). According to TI-RADS classification, 13 of these benign nodules were categorized as benign (categories 3-4a), while 6 were classified as suspicious for malignancy (categories 4b–5), as detailed in table 3.

Table 3. Distribution of benign and malignant thyroid nodules across TI-RADS categories.

TI RADS	Grade 3	Grade 4a	Grade 4b	Grade 4c	Grade 5	Total
MTN	1	2	137	32	21	193
Benign TN	5	8	6	0	0	19
Total	6	10	143	32	21	212

TI RADS diagnosis of benign MTN

As presented in table 4, among the 193 histopathologically confirmed malignant thyroid nodules (MTNs), 119 were classified as papillary microcarcinomas (≤1 cm) and 74 measured >1 cm in maximum diameter. Among the 119 microcarcinomas, 96 (80.67%) had an aspect ratio ≥1, while 23 (19.33%) had an aspect ratio <1. Microcalcifications were observed in 69 nodules (57.98%), with coarse calcifications in 4 (3.36%). Doppler ultrasound revealed grade 1 vascularity in 108 (90.76%), grade 2 in 10 (8.40%), and grade 3 in 1 (0.84%).

Table 4. Comparison of aspect ratio, calcification, and blood flow in malignant nodules of different diameters.

MTN (n=193)		Maximum Diameter ≤1cm (n=119)	Maximum Diameter >1cm (n=74)	χ^2	p-value
Aspect Ratio	≥1	96(80.67)	14(18.92)	70.988	<0.01
	<1	23(19.33)	60(81.08)		
Calcification	Non-calcified	46(38.66)	5(6.76)	36.006	<0.01
	Fine calcification	69(57.98)	51(68.92)		
	Coarse calcification	4(3.36)	18(24.32)		
Blood Flow	Grade 1	108(90.76)	50(67.57)	16.843	<0.01
	Grade 2	10(8.4)	20(27.03)		
	Grade 3	1(0.84)	4(5.40)		

In contrast, among the 74 malignant nodules >1 cm, only 14 (18.92%) exhibited an aspect ratio ≥1, while 60 (81.08%) had an aspect ratio <1. Calcification patterns included microcalcifications in 51 (68.92%) and coarse calcifications in 18 (24.32%). Vascularity was distributed as follows: grade 1 in 50 (67.57%), grade 2 in 20 (27.03%), and grade 3 in 4 (5.40%).

According to table 4, TI-RADS classification accurately identified 190 of the 193 pathologically confirmed MTNs as suspicious for malignancy (categories 4b–5), resulting in three false-negative cases (one in category 3 and two in category 4a). Among the 19 benign nodules, six were misclassified as malignant (all in category 4b), yielding six false positives. Using histopathology as the reference

standard, TI-RADS demonstrated 98.45% sensitivity, 68.42% specificity, 96.94% PPV, 81.25% NPV, and 95.75% accuracy. These metrics are summarized in table 5.

Table 5. Diagnostic performance of TI-RADS classification using histopathology as the reference standard.

	Grade 4b+4c+5 (Suspicious for Malignancy)	Grade 3+4a (Not Suspicious)	Total
Malignant by Pathological Examination	190 (True Positive)	3 (False Negative)	193
Benign by Pathological Examination	6 (False Positive)	13 (True Negative)	19
Total	196	16	212

Note: Data are presented as numbers. Sensitivity = 98.45%, Specificity = 68.42%, Positive Predictive Value = 96.94%, Negative Predictive Value = 81.25%, Accuracy = 95.75%.

DISCUSSIONS

MTNs pose significant diagnostic challenges despite advances in imaging technology [16, 17]. In this study, we validated and refined the Kwak TI-RADS system for suspicious nodules within a Chinese cohort, utilizing histopathology as the gold standard. Our findings confirm the high performance of TI-RADS in identifying MTNs aligning with previous studies that report PPVs exceeding 95% when implemented in surgical populations [18, 19]. However, rather than simply replicating previous reports, our research offers novel methodological and phenotypic insights that significantly enhance the clinical utility of ultrasound-based risk stratification.

A central aspect of our study was the consolidation of "solid composition" and "hypoechogenicity" into a unified malignancy criterion. This modification was driven by their frequent co-occurrence in malignant lesions and their overlapping pathophysiological foundations-both characteristics are associated with diminished colloid content and stromal fibrosis in papillary carcinomas [7, 20]. Kwak *et al.* notably downgraded the independent weight of "solid" components in later iterations because of their low specificity [7], suggesting redundancy between these two criteria. By integrating these elements, we streamline the scoring system while maintaining detection accuracy - an advantageous consideration in high-volume or high-suspicion contexts where prompt and reliable decision-making is critical.

Importantly, our size-stratified analysis identified distinct ultrasonographic characteristics between microcarcinomas (≤1 cm) and larger malignant nodules. Smaller thyroid carcinomas exhibited microcalcifications and irregular margins more frequently, while a taller-than-wide shape and solid/hypoechogenic architecture demonstrated greater predictive power for larger nodules [21]. This aligns with recent observations that papillary microcarcinomas may show less architectural distortion on ultrasound, which in turn makes traditional morphological criteria less sensitive [22]. These findings indicate that a uniform TI-RADS threshold may not be suitable for all nodule sizes, highlighting the necessity for context-adapted interpretation strategies.

In contrast to alternative systems like ACR-TIRADS and EU-TIRADS, which focus on standardization for general screening populations, our modified approach is tailored for a specific clinical scenario: the preoperative evaluation of nodules already classified as suspicious based on clinical or imaging criteria. While ACR-TIRADS minimizes operator dependency through rigid point-based rules, it may result in under-referral for certain high-risk subgroups [23, 24]. In contrast, our streamlined model prioritizes simplicity and high sensitivity, which are essential when the primary goal is to rule out malignancy.

While alternative diagnostic tools, such as fine-needle aspiration biopsy (FNAB), are still central to current guidelines, they have well-documented limitations, including sampling error, indeterminate cytology (e.g., Bethesda III/IV), and patient discomfort [25, 26]. Molecular testing (e.g., ThyroSeq, Afirma) can improve diagnostic yield in indeterminate cases but is costly and not widely accessible in resource-limited settings [27]. In this context, optimizing conventional ultrasound through a tailored TI-RADS application presents a cost-effective, non-invasive strategy for guiding management decisions, especially in areas with high surgical referral rates.

However, several limitations should be noted. First, the study was retrospective and conducted at a single center, which may introduce selection bias. Second, the ultrasound assessments were performed as part of routine clinical practice rather than under blinded, standardized conditions. Third, inter-observer variability in feature interpretation is a recognized challenge in TI-RADS application, although all radiologists at our institution adhere to established protocols. Future prospective studies that incorporate blinded image reviews and external validation are necessary to confirm the generalizability of our simplified scoring system.

In conclusion, our study demonstrates that targeted refinement of the Kwak TI-RADS - particularly through feature consolidation and size-specific analysis - can enhance its clinical applicability in managing suspicious thyroid nodules. These findings support the need for more individualized, phenotype-driven approaches in ultrasound-based diagnosis, providing actionable insights to improve preoperative decision-making in real-world practice.

CONCLUSION

Our study shows that the Kwak TI-RADS system

has high sensitivity (98.45%) and positive predictive value (96.94%) in identifying suspicious malignant thyroid nodules. It effectively distinguishes between malignant and benign nodules using ultrasonographic features. These findings underscore its value as a tool for preoperative risk stratification in clinically suspicious cases.

Acknowledgments: *None*.

Ethical statement: All experimental protocols in this study were approved by the Ethics Committee of The Second Hospital of Hebei Medical University (approval number: 2024-R665; approval date: 11th Oct. 2024) and conducted in accordance with the Declaration of Helsinki. Written informed consent was obtained from all individual participants.

Conflict of interest: The authors declare that they have no competing interests.

Funding: This research received no specific grant from any funding agency.

Author contributions: Y.W. and D.L., contributed to data collection; Y.Z., performed ultrasound analysis; X.X., reviewed pathology slides; Y.W., drafted the manuscript; Y.Z., X.X. and A.G., supervised the project. All authors read and approved the final version.

Data availability statement: The data supporting this study are available from the corresponding author upon reasonable request.

AI Use Statement: No artificial intelligence tools were used in the writing or editing of this manuscript.

REFERENCES

1. Han D, Zhang Y, Zhang Y, Pei Y, Huang X, Qin L, *et al.* (2025) Analysis of the detection rate and related factors of thyroid nodules in the healthy population. *Open Life Sci,* ***20****(1): 20251079*.
2. Shimura H, Yokoya S, Suzuki S, Iwadate M, Suzuki S, Matsuzuka T, *et al.* (2023) Confounding factors and biases involved in regional differences in the detection rate of thyroid cancer in the second-round thyroid ultrasound examination: the Fukushima health management survey. *J Radiat Res,* ***64****(5): 761-8*.
3. Sharma R, Kumar Mahanti G, Panda G, Singh A (2023) Thyroid nodules classification using weighted average ensemble and D-CRITIC based TOPSIS methods for ultrasound images. *Curr Med Imaging, 10.2174/1573405620666230405085358. Advance online publication. https://doi.org/10.2174/1573405620666230405085358*
4. Angell TE, Maurer R, Wang Z, Kim MI, Alexander CA, Barletta JA, *et al.* (2019) A cohort analysis of clinical and ultrasound variables predicting cancer risk in 20,001 consecutive thyroid nodules. *J Clin Endocrinol Metab,* ***104****(11): 5665-72*.
5. Wang X, Niu Y, Liu H, Tian F, Zhang Q, Wang Y, *et al.* (2025) ThyroNet-X4 genesis: an advanced deep learning model for auxiliary diagnosis of thyroid nodules' malignancy. *Sci Rep,* ***15****(1): 4214*.
6. Xia M, Song F, Zhao Y, Xie Y, Wen Y, Zhou P (2023) Ultrasonography-based radiomics and computer-aided diagnosis in thyroid nodule management: performance comparison and clinical strategy optimization. *Front Endocrinol (Lausanne),* ***14****: 1140816*.
7. Nie W, Zhu L, Yan P, Sun J (2022) Thyroid nodule ultrasound accuracy in predicting thyroid malignancy based on TIRADS system. *Adv Clin Exp Med,* ***31****(6): 597-606*.
8. Gürsel BE, Çağlar B, Özpar R, Saraydaroğlu Ö, Gökalp G, Topal NB (2024) Multimodal ultrasonography evaluation in thyroid nodule characterization: what is the ideal algorithm? *Med Ultrason,* ***26****(1): 41-9*.
9. Russ G (2016) Risk stratification of thyroid nodules on ultrasonography with the French TI-RADS: description and reflections. *Ultrasonography,* ***35****(1): 25-38*.
10. Wang Y, Lei KR, He YP, Li XL, Ren WW, Zhao CK, *et al.* (2017) Malignancy risk stratification of thyroid nodules: comparisons of four ultrasound Thyroid Imaging Reporting and Data Systems in surgically resected nodules. *Sci Rep,* ***7****(1): 11560*.
11. Kang YJ, Stybayeva G, Lee JE, Hwang SH (2022) Diagnostic performance of ACR and Kwak TI-RADS for benign and malignant thyroid nodules: An update systematic review and meta-analysis. *Cancers (Basel),* ***14****(23): 5961*.
12. Topcuoglu OM, Uzunoglu B, Orhan T, Basaran EB, Gormez A, Sarica O (2025) A real-world comparison of the diagnostic performances of six different TI-RADS guidelines, including ACR-/Kwak-/K-/EU-/ATA-/C-TIRADS. *Clin Imaging,* ***117****: 110366*.
13. Qi TY, Chen X, Liu H, Mao L, Chen J, He BL, *et al.* (2022) Comparison of thyroid nodule FNA rates recommended by ACR TI-RADS, Kwak TI-RADS and ATA guidelines. *Eur J Radiol,* ***148****: 110152*.
14. Maia FF, Matos PS, Pavin EJ, Zantut-Wittmann DE (2015) Thyroid imaging reporting and data system score combined with Bethesda system for malignancy risk stratification in thyroid nodules with indeterminate results on cytology. *Clin Endocrinol,* ***82****(3): 439-44*.
15. Weiss MH (2021) In response to "Discriminating malignancy in thyroid nodules: The nomogram versus the Kwak and ACR TI-RADS". *Otolaryngol Head Neck Surg,* ***165****(5): 755-6*.
16. Grani G, Sponziello M, Pecce V, Ramundo V, Durante C (2020) Contemporary thyroid nodule evaluation and management. *J Clin Endocrinol Metab,* ***105****(9): 2869-83*.
17. Lim JY and Kuo JH (2022) Thyroid nodule radiofrequency ablation: Complications and clinical follow up. Tech Vasc Interv Radiol, **25**(2): 100824.
18. Chen Z, Du Y, Cheng L, Zhang Y, Zheng S, Li R, *et al.* (2022) Diagnostic performance of simplified TI-RADS for malignant thyroid nodules: comparison with 2017 ACR-TI-RADS and 2020 C-TI-RADS. *Cancer Imaging,* ***22****(1): 41*.
19. Singaporewalla RM, Hwee J, Lang TU, Desai V (2017) Clinico-pathological correlation of thyroid nodule ultrasound and cytology using the TIRADS and Bethesda classifications. *World J Surg,* ***41****(7): 1807-11*.
20. Okasha HH, Mansor M, Sheriba N, Assem M, Abdelfattah Y, Ashoush OA, *et al.* (2021) Role of elastography strain ratio and TIRADS score in predicting malignant thyroid nodule. *Arch Endocrinol Metab,* ***64****(6): 735-42*.
21. Hong YR, Yan CX, Mo GQ, Luo ZY, Zhang Y, Wang Y, *et al.* (2015) Conventional US, elastography, and contrast enhanced US features of papillary thyroid microcarcinoma predict central compartment lymph node metastases. *Sci Rep,* ***5****: 7748*.
22. Jung CK, Bychkov A, Kakudo K (2022) Update from the 2022 World Health Organization classification of thyroid tumors: A standardized diagnostic approach. *Endocrinol Metab (Seoul),* ***37****(5): 703-18*.
23. Li M, Wei L, Li F, Kan Y, Liang X, Zhang H, *et al.* (2021) High risk thyroid nodule discrimination and management by modified TI-RADS. *Cancer Manag Res,* ***13****: 225-34*.
24. Fernández Velasco P, Pérez López P, Torres Torres B, Delgado E, de Luis D, Díaz Soto G (2024) Clinical evaluation of an artificial intelligence-based decision support system for the diagnosis and American College of Radiology Thyroid Imaging Reporting and Data System classification of thyroid nodules. *Thyroid,* ***34****(4): 510-8*.
25. Zhang F, Mei F, Chen W (2025) Development of a malignancy risk prediction model combining ultrasound and cytology for Bethesda category III thyroid nodules. *World J Surg Oncol,* ***23****(1): 438*.
26. Sun CF, Wu D, Sun JY, Hou YL, Xin JW, Ru XC, *et al.* (2025) Diagnostic performance of ultrasound elastography alone and in combination with conventional ultrasonography for Bethesda III-IV thyroid nodules: a systematic review and meta-analysis. *Quant Imaging Med Surg,* ***15****(10): 9613-30*.
27. Vardarli I, Tan S, Görges R, Krämer BK, Herrmann K, Brochhausen C (2024) Diagnostic accuracy of Afirma gene expression classifier, Afirma gene sequencing classifier, ThyroSeq v2 and ThyroSeq v3 for indeterminate (Bethesda III and IV) thyroid nodules: a meta-analysis. *Endocr Connect,* ***13****(7): e240170*.